

## Methylene blue binding to DNA with alternating GC base sequence: Continuum treatment of salt effects

Remo Rohs<sup>1,2</sup> and Heinz Sklenar<sup>1,\*</sup>

<sup>1</sup> Theoretical Biophysics Group, Max Delbrück Center for Molecular Medicine,  
Robert-Rössle-Str. 10, D-13092 Berlin, Germany

<sup>2</sup> Institute of Crystallography, Department of Biology, Chemistry and Pharmacy,  
Free University Berlin, Takustr. 6, D-14195 Berlin, Germany

Accepted 3 October 2000

Methylene blue (MB), an efficient singlet oxygen generating photoactive dye, binds to DNA and allows photosensitized reactions to be used for sequence-specific cleavage of the DNA backbone. Intercalation and groove binding are possible binding modes of the dye, depending on base sequences and environmental conditions. In a recent modeling study of methylene blue binding to a double stranded DNA decamer with an alternating GC sequence, six structural models for intercalation structures and for minor and major groove binding have been obtained. By estimating the binding energies (including electrostatic reaction field contributions of a salt-free aqueous solvent), symmetric intercalation at the 5'-CpG-3' and 5'-GpC-3' steps was found as the predominant binding mode, followed by a slightly weaker binding of the dye in the minor groove. In this study, the stability of the modeled structures has been analysed as a function of salt concentration. The results of finite difference numerical solutions of the non-linear Poisson-Boltzmann equation show that the stabilizing effect of salt is larger for free DNA than for the modeled MB-DNA complexes. Accordingly, the estimated binding energies decrease with increasing ionic strength. A slightly higher stabilization of the groove binding complexes results in comparable binding energies for symmetric intercalation and minor groove binding at high salt concentration. Both results are in qualitative agreement with experimental data.

### Introduction

Methylene blue (MB), a phenothiazinium dye, generates singlet oxygen very efficiently causing photooxidative damages in biological systems, including strand breakage in DNA. The photophysical behaviour of MB and its derivatives linked to single- and double-stranded oligonucleotides has been extensively studied experimentally<sup>1</sup>. The results suggest that specifically designed MB derivatives could be used as tools for site-directed cleavage of the DNA backbone. As shown by direct singlet oxygen luminescence measurements<sup>1</sup>, however, the singlet oxygen quantum yield is strongly dependent on the architecture of the dye-DNA complexes which, in turn, is affected by base sequences<sup>2</sup> and environmental conditions. An understanding of the binding behavior of MB to DNA, both in structural and energetic terms, is therefore, of considerable interest.

MB binds to poly-anionic DNA as a positively charged ligand. The planar ring system allows for

favorable stacking interactions with the base pairs, but it can also be accommodated in the grooves of the double helix. In addition to the direct electrostatic and steric interactions of the molecules, energetic contributions of solvation and desolvation including interactions with the counter ion atmosphere have an effect on the binding affinity. Our current structural knowledge is based on experimental studies, notably linear and circular dichroism (CD), carried out over the last 20 years<sup>3-8</sup>. The spectroscopic data clearly indicate intercalation of MB between two consecutive base pairs as the predominant binding mode<sup>9-12</sup>. However, neither the geometry of the intercalation complex nor the role of alternative structures as a function of base sequence and environmental conditions (ionic strength, concentration ratio) can be precisely determined on the basis of such data. A high-resolution structure of MB-DNA complexes solved by X-ray crystallography or NMR spectroscopy is not yet available.

In a recent modeling study of MB binding to a DNA decamer with alternating GC base sequence, six structural models have been derived<sup>13</sup>. This ensemble comprises two types of intercalation complexes, both for the 5'-CpG-3' and the 5'-GpC-3' site, and two

\* Author for correspondence

Phone: +4930 94062561; Fax: +49 30 94062548

Email: sklenar@mdc-berlin.de

structures with the dye inserted into the minor and major groove, respectively. A detailed energetic analysis (including an electrostatic continuum treatment of the aqueous solvent) has shown that the reaction field contributions of the solvent are critically important for predicting the relative stability of the modeled structures. In agreement with the results of CD measurements<sup>11</sup>, the estimated binding energies predict intercalation of the dye as lowest energy structures. In addition to the intercalation complexes which obey dyadic symmetry, relatively low-energy stable models involving asymmetric intercalation and groove binding complexes were located. The calculated energy differences are of the order of only a few kcal/mol and indicate that such structures could be formed under particular environmental conditions or in the case of other base sequences. The existence of both asymmetric ("gauche") intercalation complexes and groove binding complexes (in particular for AT sequences) has been discussed in several experimental studies.

Although the highly charged nucleic acids structures, are stabilized by the addition of salt, these contributions have been found in several theoretical studies<sup>14-16</sup> to be largely independent of conformational changes. Thus, the salt effect on the relative stability of different conformers can be expected to be rather small. However, the experimentally shown decrease of binding affinity for MB to DNA with increasing ionic strength<sup>17,18</sup> indicates that for absolute binding energy calculations the interactions between solute and counter ions must be taken into account. In the case of a positively charged ligand, because of the reduced total charge of the complex compared to the free DNA, the neglect of solute-salt interactions leads to an overestimation of binding energies which are calculated as energy differences between the complex and the free (DNA+MB) structures.

To estimate the salt effect on the binding behaviour of MB to DNA theoretically, we have employed the continuum approach for calculating electrostatic energies as a function of salt concentration. The calculations are based on numerical finite difference solutions of the non-linear Poisson-Boltzmann equation. The decreasing binding energy with increasing salt concentration, observed in accordance with experimental data, results from the higher stabilization of free DNA by the counter ion cloud, compared to the MB-DNA complexes. A slightly different destabilization of the intercalation and

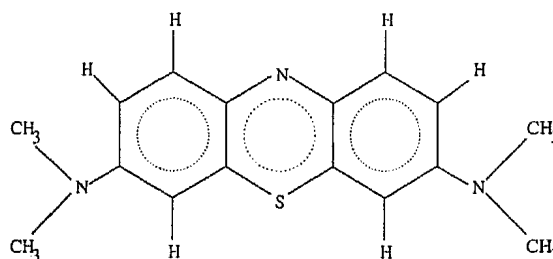


Fig. 1—Chemical structure of the MB molecule.

groove binding structures changes the relative stability of the complexes in the different binding modes, in favor of minor groove binding at high salt concentration (above 1 mole/litre).

## Materials and Methods

### Model structures

The structural models used in this work are the result of a modeling study<sup>13</sup>. The JUMNA algorithm<sup>19</sup> has been used for systematic conformational search where the force field based energy calculation was complemented by an electrostatic continuum treatment of the aqueous solvent. The chemical structure of the MB dye is depicted in Fig. 1. Six model structures, representing the different binding modes of MB to DNA, have been selected by the criterion of lowest total energies and analysed in structural terms. The most favorable intercalation complexes with lowest energies are symmetric with respect to the dyadic axis of the DNA fragment. The molecular graphics shown in Fig. 2 compare the structures obtained for the two intercalation sites, denoted by ic1-CpG and ic1-GpC. For both sites, a second local minimum was located corresponding to a rotation of the dye about the helical axis by approximately 140°. These asymmetric structures, dubbed gauche intercalation complexes, are denoted by ic2-CpG and ic2-GpC. The different stacking patterns in the symmetric and gauche intercalation complexes are compared in Fig. 3 for the 5'-GpC-3' intercalation site. The asymmetric minor groove and the symmetric major groove binding complexes, denoted by min-g and maj-g which are displayed in Fig. 4, are the lowest energy structures found by inserting the dye into the minor and major groove, respectively. Under the condition of a salt-free aqueous solution, the energetic analysis of the six model structures yielded the stability ranking: ic1-CpG = ic1-GpC > min-g > ic2-CpG = ic2-GpC > maj-g.

It should be noted that, in the present study, we have assumed that the energy-minimized structural models do not change by the addition of salt.

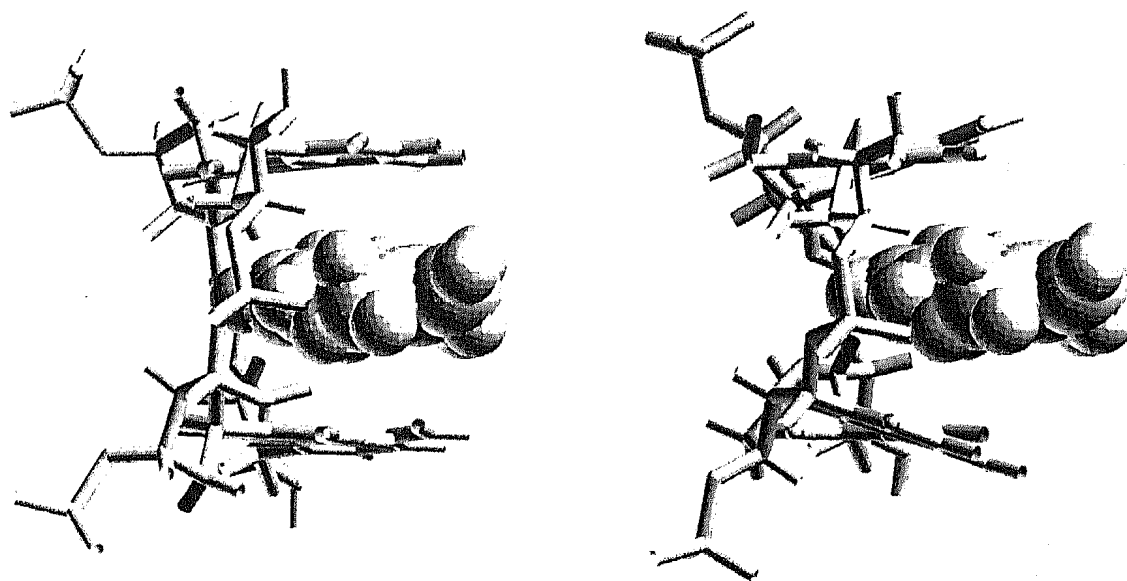


Fig. 2—Molecular graphics representations of the symmetric intercalation complexes ic1-CpG (left) and ic1-GpC (right) [Note the different propeller angles of the flanking base pairs]

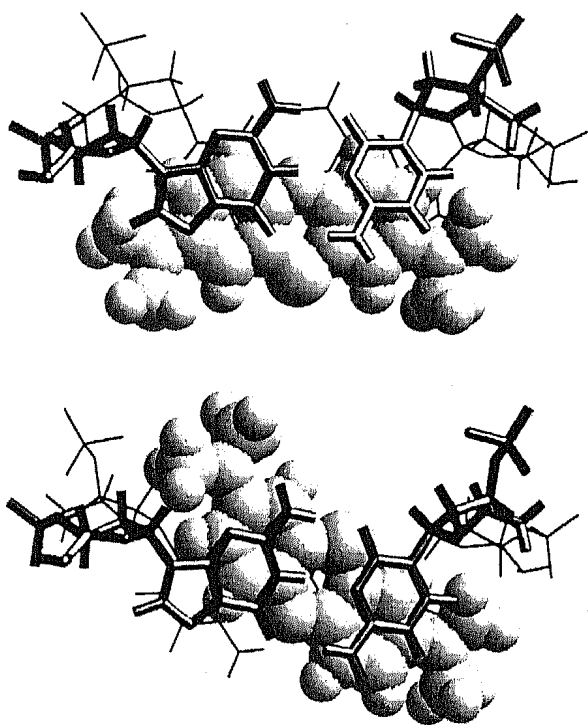


Fig. 3—Stacking pattern in the symmetric (upper figure) and asymmetric "gauche" (lower figure) intercalation complexes ic1-GpC and ic2-GpC [The view is perpendicular to the plane of the dye. In contrast to the symmetric stacking of MB on both base pairs, in the gauche intercalation complex the stacking interaction is reduced]

#### Continuum treatment of salt effects

Numerical finite difference solutions of the non-linear Poisson-Boltzmann equation for calculating electrostatic energies as a function of ion concentration were obtained by using the University of Houston Brownian Dynamics (UHBD) program<sup>20-21</sup>. The

molecular charge distributions were the same as in the reference study. The DNA fragment (containing 18 phosphate groups) carries a total charge of  $-18e$ . The total charge of MB is  $+1e$ . Partial charges on each atom of the DNA fragment were taken from the Flex force field<sup>22</sup>. The charge distribution of the MB dye was consistently defined by a Hückel-del Re procedure which has been re-parametrized on the basis of quantum chemical *ab initio* calculations<sup>13</sup>. A surface dot density of 1000 points per atom and a solvent probe radius of  $1.4 \text{ \AA}$  were used to define the solvent-inaccessible (interior) volume of the solute, which was assigned a dielectric permittivity,  $\epsilon=1.0$ . The solvent region of the box was assigned a dielectric permittivity,  $\epsilon=78.0$ . In addition, a region being accessible for the solvent but not for ions (Stern layer) was defined by assigning an ion radius,  $R=1.68 \text{ \AA}$  as proposed by Rashin & Honig<sup>23</sup>. The dielectric boundary smoothing option was employed to reduce the grid-dependence of the calculated electrostatic energies. Three-stage focusing calculations were performed with a grid spacing of  $< 0.33 \text{ \AA}$  for the final grid ( $120^3$  grid points). The electrostatic free energy was calculated from a volume integral over all space using the formula<sup>24</sup>:

$$E_{elec} = \int [\rho^f \Phi / 2 - \rho^m \Phi / 2 - \Delta \Pi] dv$$

where  $\rho^f$  and  $\rho^m$  are the distribution of fixed and mobile (ionic) charges, respectively.  $\Phi$  is the electrostatic potential and  $\Delta \Pi$  is an osmotic pressure term due to the excess ion concentration at any point given by  $\Delta \Pi = kT c (2 \cosh(\Phi) - 2)$  where  $c$  is the monovalent ion concentration.

### Results and Discussion

Electrostatic energies of the six modeled complex structures and of the free DNA fragment and MB molecule were calculated as a function of monovalent salt concentration between  $10^{-4}$  moles/litre and 2 moles/litre. The energies given in Table 1 are relative to the corresponding values of electrostatic energies for zero salt concentration. The data clearly show a significantly higher stabilization of free (DNA+MB) by the addition of salt than it is observed for the MB-

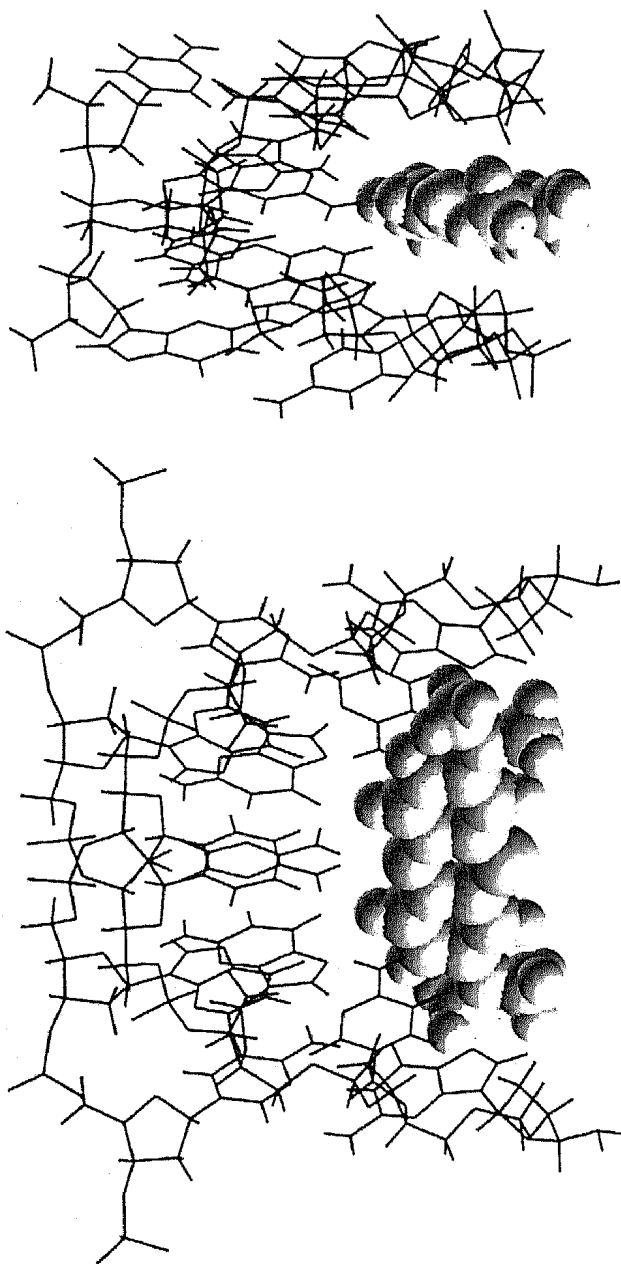


Fig. 4—Structural models obtained for minor (upper figure) and major (lower figure) groove binding of MB to DNA [Whereas the long axis of the dye is oriented parallel to the strands in the minor groove complex, it spans the groove in the major groove complex]

DNA complexes. The difference is presumably due to the change of the total charge which is by one unit lower in the complex than for free DNA. This interpretation is supported by a study on the salt dependence obtained for binding of a negatively charged ligand to RNA, where reversely the increase of the total charge yielded a higher stability of the complex with increasing salt concentration<sup>25</sup>.

Total energies of the different structures were obtained by adding the non-electrostatic energy contributions to the calculated electrostatic energies. For each of the structures, this component, calculated as the sum of non-bonded atom-atom Lennard-Jones potentials and angle-dependent terms, is salt-independent and has been taken from the results of the former modeling study. The results given in Fig. 5 as a plot vs. the decadic logarithm of ionic strength show directly the relative stability of the different complex structures in comparison with the free (DNA+MB) structure. The total energy of the symmetric intercalation complex ic1-CpG, which was found as the lowest energy structure at zero salt concentration, has been chosen as the zero point of the energy scale. The relative stability of the different complex structures is only slightly affected by the addition of salt. The prediction of symmetric intercalation complexes at the 5'-CpG-3' and the 5'-GpC-3' sites is therefore independent of salt concentration, in accordance with spectroscopic data on MB binding to a GC alternating base sequence<sup>11,12</sup>. In addition, with this result we expect only very small changes in the model structures if the electrostatic continuum treatment of salt effect is included in the computationally demanding conformational search and energy minimization procedure. Therefore, it gives a justification for the "single point" correction we have used in our simplified approach.

A little higher stabilization of the groove binding complexes by the ionic atmosphere leads to a comparable stability of the minor groove binding complex and the symmetric intercalation complexes at high ion concentration above 1 mole/litre. However, we should note that for high ion concentrations, the results of the continuum treatment become questionable because of the neglect of ion-ion correlations by the Debye-Hückel approximation which is the basis of the Poisson-Boltzmann equation.

The binding energies given in Table 2 and shown in Fig. 6 as a function of ionic strength were estimated by the differences between the calculated total energies of the respective complex structures and the

free (DNA+MB) structure for fixed ion concentrations. The overall lowering of the binding energies by the addition of salt is in agreement with experimental results<sup>18</sup>. In addition to the slight favouring of groove binding complexes discussed above, the data also indicate a small sequence effect by comparing intercalations at the 5'-CpG-3' and 5'-

GpC-3' steps. In this case, the salt effect induces a small shift of the relative stability in favor of 5'-GpC-3' intercalation.

### Acknowledgement

The authors would like to thank B. Jayaram for valuable discussions. R. Rohs acknowledges a

Table 1—Electrostatic free energies  $\Delta E_{elec}$  (in kcal/mol) obtained for the modeled structures as a function of monovalent salt concentration (in moles/litre). [The energies are given relative to the values for zero salt concentration]

Structure	0.0	0.0001	0.001	0.01	0.1	0.5	1.0	2.0
ic1-CpG	0.0	-7.6	-20.0	-36.0	-50.8	-57.9	-60.0	-61.7
ic1-GpC	0.0	-8.0	-20.6	-36.6	-51.5	-58.6	-60.8	-62.5
ic2-CpG	0.0	-7.7	-20.2	-36.2	-51.0	-58.1	-60.2	-61.9
ic2-GpC	0.0	-7.9	-20.4	-36.4	-51.2	-58.3	-60.5	-62.2
min-g	0.0	-8.7	-21.5	-37.7	-52.7	-60.1	-62.4	-64.2
maj-g	0.0	-8.2	-21.0	-37.3	-52.3	-59.8	-62.0	-63.8
free (DNA+MB)	0.0	-10.9	-25.5	-43.3	-59.8	-68.0	-70.5	-72.2

Table 2—Estimated binding energies  $E_{Bdg}$  (in kcal/mol) of the modeled MB-DNA complexes as a function of salt concentration (in moles/litre)

Structure	0.0	0.0001	0.001	0.01	0.1	0.5	1.0	2.0
ic1-CpG	-14.8	-11.5	-9.3	-7.5	-5.8	-4.7	-4.3	-4.0
ic1-GpC	-14.7	-11.8	-9.8	-8.0	-6.4	-5.3	-5.0	-4.7
ic2-CpG	-12.2	-9.0	-6.9	-5.1	-3.4	-2.3	-1.9	-1.6
ic2-GpC	-12.4	-9.4	-7.3	-5.5	-3.8	-2.7	-2.4	-2.1
min-g	-12.8	-10.6	-8.8	-7.2	-5.7	-4.9	-4.7	-4.5
maj-g	-10.3	-7.6	-5.8	-4.3	-2.8	-2.1	-1.8	-1.6

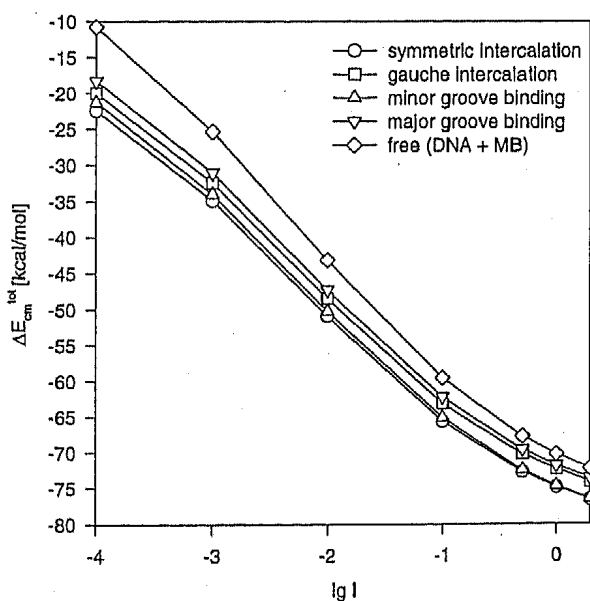


Fig. 5—Total Energies  $\Delta E_{cm}^{tot}$  (in kcal/mol) of the modeled structures as a function of the decadic logarithm of ionic strength  $I$  (in moles/litre) [For the sake of clarity, the energies of the different intercalation structures at the CpG and GpC steps are averaged]

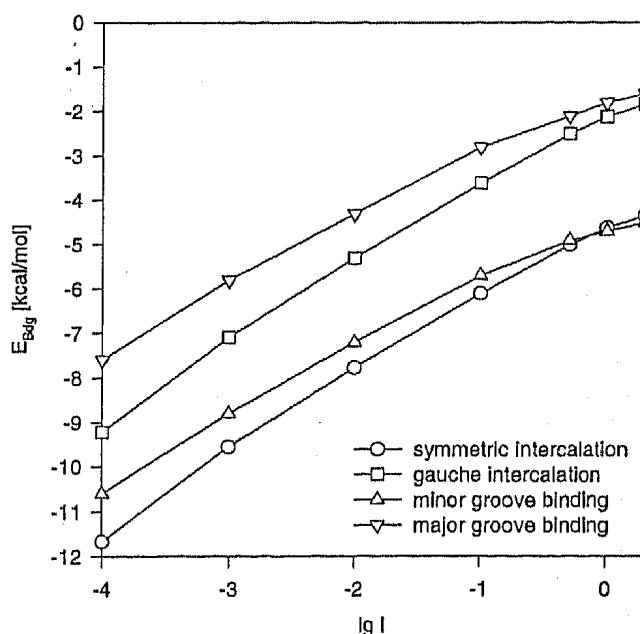


Fig. 6—Estimated binding energies of the modeled MB-DNA complexes vs. the decadic logarithm of ionic strength (in moles/litre) [The binding energies of the different intercalation structures at the CpG and GpC steps are averaged]

IUPAB/UNESCO travel fellowship for visiting the XIIIth International Biophysics Congress in India and funding by the Deutsche Forschungsgemeinschaft (DFG-GK 80).

### References

- 1 Rohs R (1997) *Spektroskopische Untersuchungen und theoretische Modellierungen physikalischer Eigenschaften von Farbstoff-Oligonukleotid-Konjugaten*, Diploma Thesis, Humboldt University Berlin
- 2 Kelly J M, van der Putten W J M & McConnell D J (1987) *Photochem Photobiol* 45 (2), 167-175
- 3 Tuite E M & Kelly J M (1993) *J Photochem Photobiol B* 21, 103-124
- 4 Nordén B & Tjernelid F (1982) *Biopolymers* 21, 1713-1734
- 5 Wang J, Hogan M & Austin R H (1982) *Proc Natl Acad Sci USA* 79, 5896-5900
- 6 Hogan M, Wang J, Austin R H, Monitto C L & Hershkowitz S (1982) *Proc Natl Acad Sci USA* 79, 3518-3522
- 7 Lyng R, Hård T & Nordén B (1987) *Biopolymers* 26, 1327-1345
- 8 Bradley D F, Stellwagen N C, O'Konski C T & Paulson C M (1972) *Biopolymers* 11, 645-652
- 9 Müller W & Crothers D M (1975) *Eur J Biochem* 54, 267-277
- 10 OhUigin C, McConnell D J, Kelly J M & van der Putten W J M (1987) *Nucleic Acids Research* 15, 7411-7427
- 11 Tuite E M & Nordén B (1994) *J Am Chem Soc* 116, 7548-7556
- 12 Tuite E M & Kelly J M (1995) *Biopolymers* 35, 419-433
- 13 Rohs R, Sklenar H, Lavery R & Röder B (2000) *J Am Chem Soc* 122, 2860-2866
- 14 Zakrzewska K, Madami A & Lavery R (1996) *Chem Phys* 204, 263-269
- 15 Zacharias M & Sklenar H (1997) *Biophys J* 73, 2990-3003
- 16 Zacharias M & Sklenar H (1999) *J Mol Biol* 289, 261-275
- 17 van der Putten W J M & Kelly J M (1989) *Photochem Photobiol* 49 (2), 145-151
- 18 Hagmar P, Pierrou S, Nielsen P, Nordén B & Kubista M (1992) *J Biomol Struct Dyn* 9, 667-679
- 19 Lavery R, Zakrzewska K & Sklenar H (1995) *Comput Phys Commun* 91, 135-158
- 20 Davis M E, Madura J D, Luty B A & McCammon J A (1991) *Comput Phys Commun* 62, 187-198
- 21 Madura J D, Davis M E, Wade R, Luty B A, Ilin A, Antosiewicz A, Gilson, M K, Bagheri B, Ridgway Scott L & McCammon J A (1995) *Comput Phys Commun* 91, 57-95
- 22 Lavery R, Sklenar H, Zakrzewska K & Pullman B (1986) *J Biomol Struct Dynam* 3, 989-1014
- 23 Rashin A A & Honig B (1985) *J Phys Chem* 89, 5588-5593
- 24 Sharp K A & Honig B (1990) *J Phys Chem* 94, 7684-7692
- 25 Maier A (2000) *Konformationsanalyse von RNA-Strukturmotiven mit Methoden der molekularen Modellierung*, Ph D Thesis, Free University Berlin